

Synthesis and luminescence properties of $\text{ZrO}_2:\text{Gd}^{3+}$, RE^{3+} ($\text{RE} = \text{Sm}^{3+}$, Er^{3+}) phosphors

ESRA YILDIZ*

Bozok University, Department of Chemistry, 66900 Yozgat, Turkey

In the present study, ZrO_2 co-doped with $\text{Gd}^{3+}/\text{Sm}^{3+}$ and $\text{Gd}^{3+}/\text{Er}^{3+}$ ions have been synthesized using Pechini method. Phase composition, morphology and photoluminescence properties of the synthesized phosphors were investigated by using X-ray powder diffraction (XRD), differential thermal analysis/thermal gravimetry (DTA/TG), scanning electron microscopy (SEM) and photoluminescence spectrofluorometer (PL). After heating at 1200 °C, XRD revealed that the phosphors were crystallized as monoclinic and tetragonal multiphases. SEM images indicated that the phosphors consist of fine and spherical grains with a size around 200 nm to 250 nm. Luminescence studies of these phosphors have been carried out on the emission and excitation, along with lifetime measurements.

Keywords: ZrO_2 ; Sm^{3+} ; Er^{3+} ; luminescence

1. Introduction

Zirconium oxide (ZrO_2) is one of the widely studied oxide materials over the last two decades because of its excellent electrical and optical properties, such as high dielectric constant (ranging from 23 to 29), good thermal stability, high melting point, and wide band gap (5 eV to 7 eV) [1, 2]. Due to its excellent optical properties, such as high refractive index, large optical band gap, low optical loss and high transparency in the visible and near infrared region [3, 4], it is widely used as an essential material in the optical fields including broadband interference filters and active electro-optical devices. ZrO_2 is an ideal host material for various phosphors, because of its wide band-gap and low phonon energy [5].

The intrinsic luminescence of zirconia is relatively weak and therefore, for practical luminescence applications, zirconia is doped with rare earth (RE) ions [6]. Wide-band gap materials doped with RE ions have been already commercialized as luminescent phosphors. The basis for these new applications was provided by the high quantum yield of intra-shell emission in the case of RE

or transition metal ions. Rare earth ions have been playing an important role in modern lighting and display fields due to the abundant emission of colors based on their 4f-4f or 5d-4f transitions [7]. To be excited efficiently, phosphors activated with rare earth ions should have a strong and broad absorption band in the UV or VUV region depending on the practical application requirements [7, 8].

Sol-gel technology, by which composite organic, inorganic materials are made at relatively low temperature, involves the hydrolysis of the constituent molecular precursors and subsequent polycondensation to glass-like form [9]. Sol-gel methods enable homogenous samples to be obtained at low temperatures and the starting cationic composition to be maintained by using metal salts as raw materials and mixing them in a liquid solution. The most obvious advantage of this sol-gel method is that reagents are mostly mixed at atomic level, which may increase the reaction rate and decrease the synthesis temperature. In 1967, Pechini [10] developed a process for the preparation of precursor polymeric resin. In this process, first, a mixture of cations is formed using organic agents, such as citric acid (CA) or ethylenediaminetetraacetic acid (EDTA) and ethylene glycol (EG). Second, the cations take a chelate and

*E-mail: esra.korkmaz@bozok.edu.tr

the polymeric resin forms. Finally, this polymer decomposes at 573 K. Two reactions are involved in the formation of a complex between citric acid or EDTA and metals, and esterification between citric acid or EDTA and ethylene glycol (EG). The aim of the polymeric organic net obtained by esterification is to reduce any segregation of the cations [11].

In this paper, $\text{ZrO}_2:\text{Gd}^{3+}-\text{Sm}^{3+}$ and $\text{ZrO}_2:\text{Gd}^{3+}-\text{Er}^{3+}$ phosphors have been prepared by Pechini method using ethylene glycol and citric acid as a chelating agent. The synthesized phosphors were characterized by DTA/TG, XRD and SEM. After synthesis and characterization of the phosphors, the photoluminescence properties were investigated using a spectrofluorometer at room temperature.

2. Experimental

2.1. Powder synthesis

$\text{Gd}^{3+}/\text{Sm}^{3+}$ and $\text{Gd}^{3+}/\text{Er}^{3+}$ co-doped zirconia phosphors were prepared by Pechini method. Powders of ZrCl_4 , $\text{Gd}(\text{NO}_3)_3 \cdot 6\text{H}_2\text{O}$, $\text{Sm}(\text{NO}_3)_3 \cdot 6\text{H}_2\text{O}$ and $\text{Er}(\text{NO}_3)_3 \cdot 5\text{H}_2\text{O}$ were used as starting materials. The initial compositions were $98\text{ZrO}_2 \cdot 1\text{Gd}_2\text{O}_3 \cdot 1\text{Sm}_2\text{O}_3$ ($\text{ZrO}_2:1\% \text{Gd}^{3+}$, $1\% \text{Sm}^{3+}$) and $98\text{ZrO}_2 \cdot 1\text{Gd}_2\text{O}_3 \cdot 1\text{Er}_2\text{O}_3$ ($\text{ZrO}_2:1\% \text{Gd}^{3+}$, $1\% \text{Er}^{3+}$). The powders were dissolved in distilled water under stirring. All the cation solutions and citric acid were mixed well in the stoichiometric ratio. The weight ratio of the total metal cations ($\text{Zr} + \text{Gd} + \text{Sm}$ and $\text{Zr} + \text{Gd} + \text{Er}$) to citric acid was 1:4. After that, ethylene glycol (EG) was dropped into the continually stirred solution. The molar ratio of citric acid to ethylene glycol was 1:4. The solution was stirred on a hot plate at a temperature of 80 °C for 4 h and then a transparent gel was formed. The resulting gel was dried at 120 °C for 24 h in air. The dried gels were heated at 900 °C for 12 h to decompose the organic components. The obtained precursor was then finely ground in a mortar and sintered at 1100 °C and 1200 °C for 12 h, respectively.

2.2. Characterization

The phase structure studies were performed by X-ray powder diffraction (Philips PANalytical, Empyrean) operating at $\text{CuK}\alpha$ radiation (45 kV, 40 mA). The thermal behavior of the phosphors was evaluated by thermal gravimetry (TG) and differential thermal analysis (DTA) using a PerkinElmer diamond analyzer in the temperature range of 50 °C to 1000 °C under inert N_2 atmosphere at the heating rate of 10 °C/min. The crystallite size verification and morphology studies were performed using a LEO 440 model scanning electron microscope operated at 20 kV. The photoluminescence (PL) excitation and emission spectra were measured by Photon Technology International Quanta Master 30 model phosphorescence/fluorescence spectrofluorometer equipped with a pulsed xenon lamp.

3. Results and discussion

3.1. Structural and morphological characterization

The XRD patterns of obtained $\text{ZrO}_2:1\% \text{Gd}^{3+}$, $1\% \text{Sm}^{3+}$ and $\text{ZrO}_2:1\% \text{Gd}^{3+}$, $1\% \text{Er}^{3+}$ phosphors sintered at 1200 °C for 12 h are given in Fig. 1. The observed XRD pattern peaks were indexed and compared with ZrO_2 monoclinic (m) phase (JCPDS Card No. 01-078-1807) and ZrO_2 tetragonal (t) phase (JCPDS Card No. 01-080-2155). It was found that the phosphors are mostly monoclinic and tetragonal multiphase.

The DTA/TG curves of $\text{ZrO}_2:1\% \text{Gd}^{3+}$, $1\% \text{Sm}^{3+}$ phosphor are shown in Fig. 2. As seen in the DTA curve, no endothermic or exothermic peak is observed in the range between room temperature and 1000 °C. This observation reveals that in the formed samples no phase transition took place and they showed a high thermal stability up to around 1000 °C. This result is in agreement with the measured ones. There is no mass loss between 50 °C and 1000 °C as shown in the TG curve. The DTA/TG curve of the $\text{ZrO}_2:1\% \text{Gd}^{3+}$, $1\% \text{Er}^{3+}$ phosphor is quite similar to the curves shown in this figure.

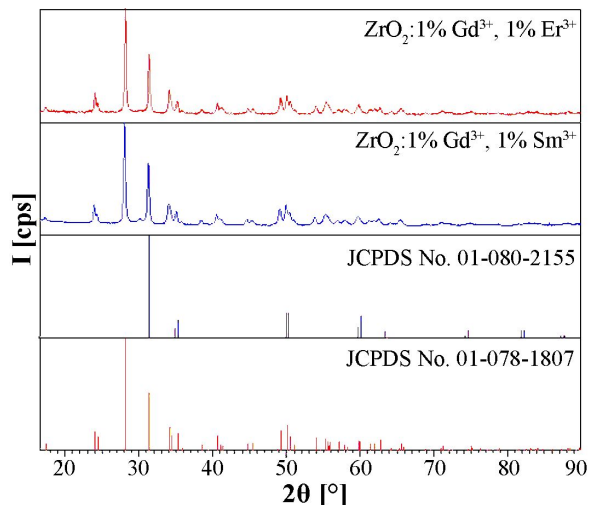


Fig. 1. XRD patterns of $\text{ZrO}_2:1\% \text{Gd}^{3+}, 1\% \text{Sm}^{3+}$ and $\text{ZrO}_2:1\% \text{Gd}^{3+}, 1\% \text{Er}^{3+}$ phosphors calcined at $1200\text{ }^\circ\text{C}$ for 12 h.

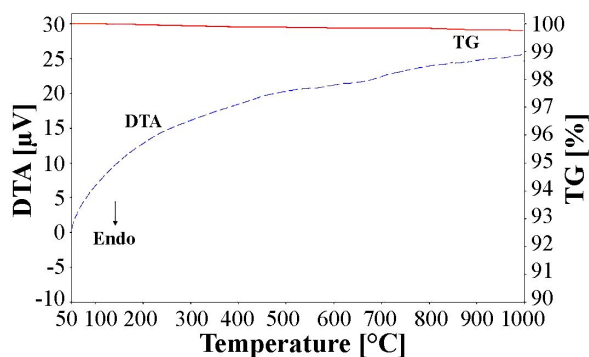


Fig. 2. DTA/TG curves of $\text{ZrO}_2:1\% \text{Gd}^{3+}, 1\% \text{Sm}^{3+}$.

In order to examine the surface morphology and particle sizes of the synthesized material, SEM images were taken. Fig. 3 shows SEM images of the as-prepared $\text{ZrO}_2:1\% \text{Gd}^{3+}, 1\% \text{Sm}^{3+}$ and $\text{ZrO}_2:1\% \text{Gd}^{3+}, 1\% \text{Er}^{3+}$ phosphors obtained by Pechini method at $1200\text{ }^\circ\text{C}$ for 12 h. The presented micrographs show that the phosphors consist of regular fine grains and the particle size is between 200 nm and 250 nm.

3.2. Luminescence properties

Fig. 4 shows the excitation and emission spectra of $\text{ZrO}_2:1\% \text{Gd}^{3+}, 1\% \text{Sm}^{3+}$ phosphor excited at 405 nm and monitored at 623 nm, respectively. It exhibits a broad excitation band in the range

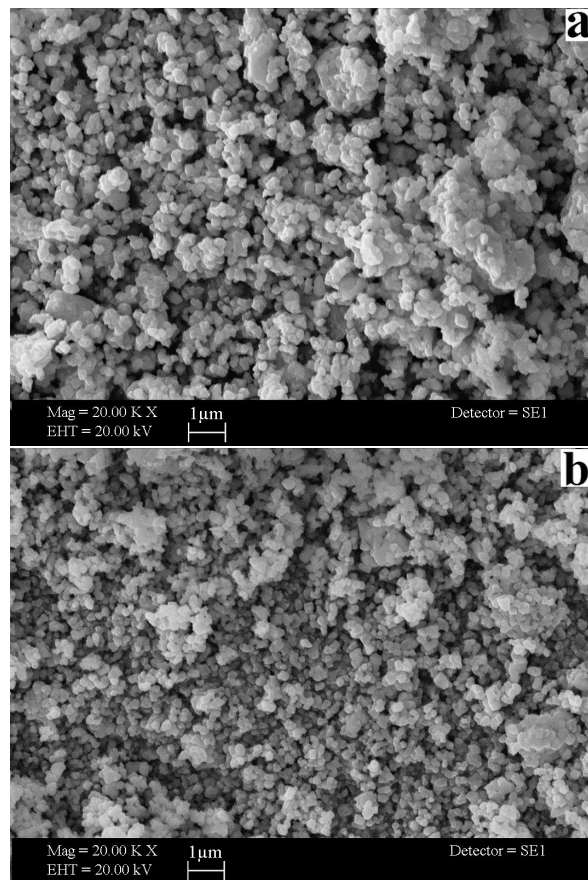


Fig. 3. The measured SEM images of (a) $\text{ZrO}_2:1\% \text{Gd}^{3+}, 1\% \text{Sm}^{3+}$ and (b) $\text{ZrO}_2:1\% \text{Gd}^{3+}, 1\% \text{Er}^{3+}$ phosphors.

of 235 nm to 320 nm which is attributable to the charge transfer (CT) band because an electron is transferred from the oxygen 2p orbital to the empty 4f orbital of samarium [12]. The sharp excitation lines between 350 nm and 500 nm are related to the $4f^5 - 4f^5$ transitions of Sm^{3+} in the host. The excitation spectrum, consists of three bands originating from the ${}^6\text{H}_{5/2} \rightarrow {}^4\text{D}_{3/2}$ (370 nm), ${}^6\text{H}_{5/2} \rightarrow {}^4\text{F}_{7/2}$ (405 nm) and ${}^6\text{H}_{5/2} \rightarrow {}^4\text{I}_{11/2}$ (474 nm) transitions of the Sm^{3+} ions [13]. From all these transitions, the transition at ${}^6\text{H}_{5/2} \rightarrow {}^4\text{F}_{7/2}$ at wavelength 405 nm shows the strongest intensity.

Photoluminescence emission spectrum was measured in the range of 450 nm to 900 nm under the 405 nm excitation. It consists of the intra f-f transition lines within the Sm^{3+} ions. When the

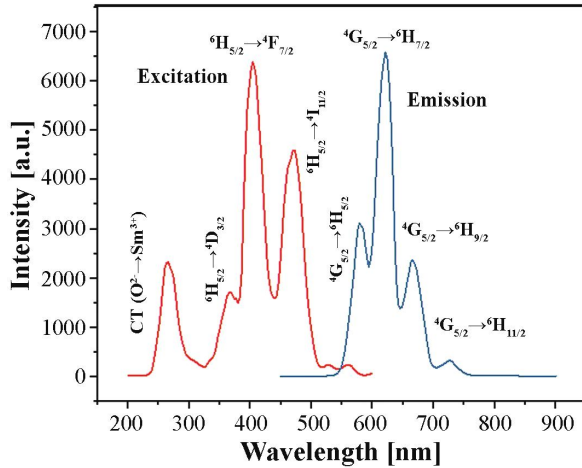


Fig. 4. Excitation and emission spectra of $\text{ZrO}_2:1\% \text{Gd}^{3+}$, $1\% \text{Sm}^{3+}$ phosphor.

Sm^{3+} ions are excited to $^4\text{F}_{7/2}$ level (405 nm), initially they relax to the $^4\text{G}_{5/2}$ level by nonradiative relaxation (NR) process as shown in Fig. 5. Since there are several energy levels available between $^4\text{F}_{7/2}$ and $^4\text{G}_{5/2}$ levels, this could help to have efficient NR. In this NR process the $^4\text{G}_{5/2}$ luminescence level is populated. The relaxation of Sm^{3+} ions leads to four characteristic emission bands observed at 579 nm, 620 nm, 665 nm and 726 nm. They are assigned to the $^4\text{G}_{5/2} \rightarrow ^6\text{H}_j$ transitions of Sm^{3+} ions, where $J = 5/2, 7/2, 9/2$ and $11/2$, respectively [14–17]. There are no excitation and emission bands of Gd^{3+} . Because of the overlap of energy levels of both Sm^{3+} and Gd^{3+} in the UV region, it is really difficult to differentiate more accurately in labeling the levels of Gd^{3+} ions.

The excitation and emission spectra of the $\text{ZrO}_2:1\% \text{Gd}^{3+}$, $1\% \text{Er}^{3+}$ phosphor powders sintered at 1200°C at room temperature are given in Fig. 6. Two bands are observed at 275 nm and 313 nm in the excitation spectrum ($\lambda_{\text{em}} = 635 \text{ nm}$). The excitation bands are related to the f-f transitions of Gd^{3+} in ZrO_2 , which correspond to the $^8\text{S}_{7/2} \rightarrow ^6\text{I}_{11/2}$ and $^8\text{S}_{7/2} \rightarrow ^6\text{P}_{7/2}$, respectively [18]. The emission spectrum ($\lambda_{\text{ex}} = 275 \text{ nm}$) shows one strong band at 635 nm due to the $^6\text{I}_{7/2} \rightarrow ^6\text{P}_{3/2}$ transition of Gd^{3+} [19]. The much weaker violet and green emission bands located at 410, 475 and 565 nm, are ascribed

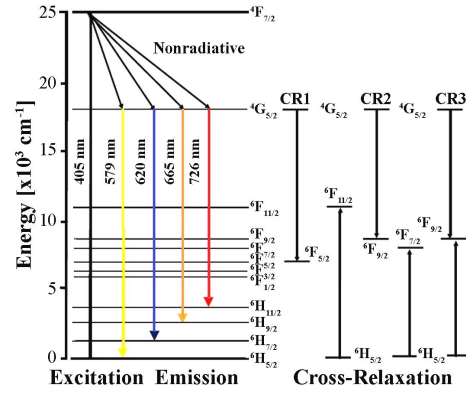


Fig. 5. Partial energy levels diagram of the Sm^{3+} doped ZrO_2 showing excitation, emission and cross-relaxation channels.

to the $^2\text{G}_{9/2} \rightarrow ^4\text{I}_{15/2}$, $^4\text{F}_{7/2} \rightarrow ^4\text{I}_{15/2}$ and $^4\text{S}_{3/2} \rightarrow ^4\text{I}_{15/2}$ transitions of Er^{3+} ions [20]. $\text{ZrO}_2:1\% \text{Gd}^{3+}$, $1\% \text{Er}^{3+}$ shows that the strongest emission peak is located at 635 nm, which is closer to the red range.

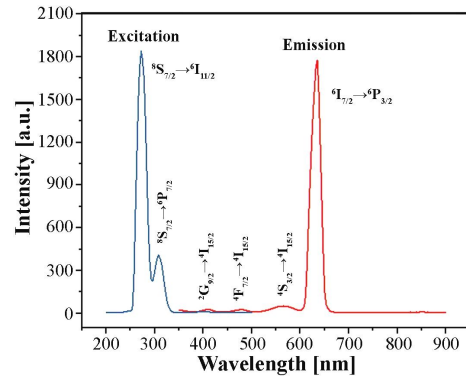


Fig. 6. Excitation and emission spectra of $\text{ZrO}_2:1\% \text{Gd}^{3+}$, $1\% \text{Er}^{3+}$.

Fig. 7 shows PL decay curves of the $\text{ZrO}_2:1\% \text{Gd}^{3+}$, $1\% \text{Sm}^{3+}$ and $\text{ZrO}_2:1\% \text{Gd}^{3+}$, $1\% \text{Er}^{3+}$ phosphors. The luminescence decay curve fitted well by a decay time can be calculated by a single exponential function represented as:

$$I = A_1 \exp(-t/\tau_1) + C \quad (1)$$

where I is phosphorescence intensity, A_1 and C are constants, t is time, τ_1 is life time for the exponential components. The decay lifetimes τ_1 for the exponential components of the $\text{ZrO}_2:1\% \text{Gd}^{3+}$, 1%

Sm^{3+} and $\text{ZrO}_2:1\% \text{Gd}^{3+}, 1\% \text{Er}^{3+}$ phosphors were found as 112.9 μs and 78.7 μs , respectively. The phosphor $\text{ZrO}_2:1\% \text{Gd}^{3+}, 1\% \text{Sm}^{3+}$ shows much longer afterglow than the $\text{ZrO}_2:1\% \text{Gd}^{3+}, 1\% \text{Er}^{3+}$ phosphors which indicates that Er^{3+} ions do not play an important role in prolonging the afterglow.

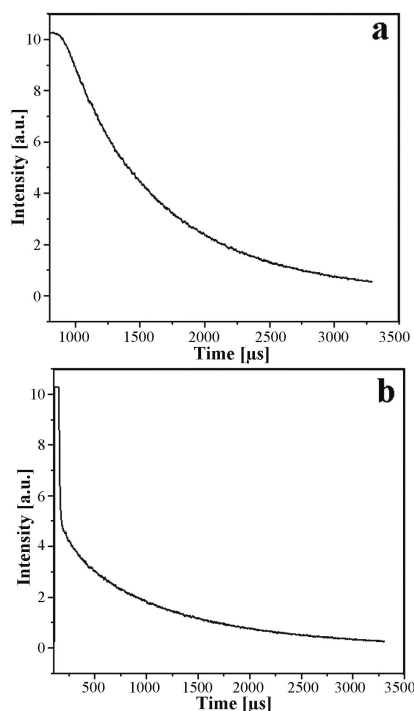


Fig. 7. The decay curves of (a) $\text{ZrO}_2:1\% \text{Gd}^{3+}, 1\% \text{Sm}^{3+}$ and (b) $\text{ZrO}_2:1\% \text{Gd}^{3+}, 1\% \text{Er}^{3+}$ phosphors.

4. Conclusions

In summary, it is concluded that the novel $\text{ZrO}_2:1\% \text{Gd}^{3+}, 1\% \text{Sm}^{3+}$ and $\text{ZrO}_2:1\% \text{Gd}^{3+}, 1\% \text{Er}^{3+}$ phosphors have successfully been synthesized by using Pechini method, which is known to be effective and simple, and their photoluminescence properties were investigated. The $\text{ZrO}_2:1\% \text{Gd}^{3+}, 1\% \text{Er}^{3+}$ and $\text{ZrO}_2:1\% \text{Gd}^{3+}, 1\% \text{Sm}^{3+}$ phosphors were excited by the ultraviolet and light of near ultraviolet, respectively. The PL analysis showed that all of the activated systems, which were based on same

host/activator and the different co-activator, exhibit excitations and red emissions due to f-f transitions of $\text{Gd}^{3+}/\text{Sm}^{3+}$ and $\text{Gd}^{3+}/\text{Er}^{3+}$. Also, the Sm^{3+} ions co-doped phosphor showed a longer lifetime than Er^{3+} ions co-doped phosphor. Therefore, $\text{ZrO}_2:1\% \text{Gd}^{3+}, 1\% \text{Sm}^{3+}$ may be a good candidate for red phosphors.

References

- [1] LIAO L., BAI J.W., LIN Y.C., YQ Q.U., HUANG Y., DUAN X.F., *Adv. Mater.*, 22 (2015), 1941.
- [2] WANG S.J., ONG C.K., *Appl. Phys. Lett.*, 80 (2002), 2541.
- [3] JOHN BERLIN I., LAKSHMI J.S., SUJATHA LEKSHMY S., DANIEL G.B., THOMAS P.V., JOY K., *J. Sol-gel Sci. Technol.*, 58 (2011), 669.
- [4] JOHN BERLIN I., MANEESHYA L.V., JIJIMON K., THOMAS P.V., JOY K., *J. Lumin.*, 132 (2012), 3077.
- [5] JOHN BERLIN I., ANITHA V.S., THOMAS P.V., JOY K., *J. Sol-gel Sci. Technol.*, 64 (2012), 289.
- [6] SMITS K., GRIGORJEVA L., MILLERS D., SARAKOVSKIS A., OPALINSKA A., FIDELUS J.D., LOJKOWSKI W., *Opt. Mater.*, 32 (2010), 827.
- [7] BLASSE G., GRABMAIER B.C., *Luminescent Materials*, Springer, Berlin Heidelberg, 1994.
- [8] FELDMANN C., JUSTEL T., RONDA C.R., SCHMIDT P.J., *Adv. Funct. Mater.*, 13 (2003), 511.
- [9] REISFELD R., JORGENSEN C.K., *Structure and bonding*, Springer-Verlag, Heidelberg, 1992.
- [10] PECHINI M.P., US Patent No. 3.330.697, July 1, 1967.
- [11] VAQUEIRO P.P., LOPEZ-QUINTELA M.A., *Chem Mater.*, 9 (1997), 2836.
- [12] LIN H., PUN E.Y.B., WANG X., LIU X., *J. Alloy Compd.*, 390 (2005), 197.
- [13] KINDRAT I.I., PADLYAK B.V., DRZEWIECKI A., *J. Lumin.*, 166 (2015), 264.
- [14] SOBCZYK M., *Spectrochim. Acta A*, 149 (2015), 965.
- [15] DENG H., ZHAO Z., WANG J., HE Z., LI M., NOH H.M., JEONG J.H., YU R., *J. Solid State Chem.*, 228 (2015), 110.
- [16] LUITEL H.N., WATARI T., CHAND R., TORIKAI T., YADA M., *Opt. Mater.*, 34 (2012), 1375.
- [17] YANG Z., DONG H., LIU P., HOU C., LIANG X., WANG C., LU F., *J. Rare Earths*, 32 (2014), 404.
- [18] CARNALL W.T., GOODMAN G.L., RAJNAK K., RANA R.S.A., *J. Chem. Phys.*, 90 (1989), 3443.
- [19] WEGH R.T., DONKER H., MAIJERINK A., LAMMINMAKI R.J., HOLSA J., *Phys. Rev. B*, 56 (1997), 13841.
- [20] WANG G., QIN W., WANG L., WEI G., ZHU P., ZHANG D., DING F., *J. Rare Earths*, 27 (2009), 394.

Received 2017-10-12

Accepted 2018-03-14